Acta Crystallographica Section D
Biological Crystallography
ISSN 0907-4449

Structure of rabbit-muscle glyceraldehyde-3-phosphate dehydrogenase

Sandra W. Cowan-Jacob,[a] Markus Kaufmann,[b]† Anthony N. Anselmo,[c] Wilhelm Stark[a] and Markus G. Grütter[b]*

[a]Novartis Pharma AG, Core Technology Area, Analytics and Biomolecular Structure, CH-4002 Basel, Switzerland, [b]Institute of Biochemistry, University of Zurich, Winterthurerstrasse 190, CH-8057 Zürich, Switzerland, and [c]University of Texas, Southwestern Medical Centre at Dallas, Department of Cell Biology, 5323 Harry Hines Boulevard, Dallas, Texas 75390-9162, USA

† Current address: University of California Los Angeles UCLA-DOE Institute for Genomics and Proteomics, Molecular Biology Institute, 225 Boyer Hall, Box 951570, Los Angeles, CA 90095-1570, USA.

Correspondence e-mail: gruetter@bioc.unizh.ch

Received 11 December 2002
Accepted 16 September 2003

PDB Reference: rabbit-muscle glyceraldehyde-3-phosphate dehydrogenase, 1j0x, r1j0xsf.

The crystal structure of the tetrameric form of D-glyceraldehyde-3-phosphate dehydrogenase (GAPDH) isolated from rabbit muscle was solved at 2.4 Å resolution after careful dynamic light-scattering experiments to find a suitable buffer for crystallization trials. The refined model has a crystallographic *R* factor of 20.3%. Here, the first detailed model of a mammalian GAPDH is presented. The cofactor NAD^+ (nicotinamide adenine dinucleotide) is bound to two subunits of the tetrameric enzyme, which is consistent with the negative cooperativity of NAD^+ binding to this enzyme. The structure of rabbit-muscle GAPDH is of interest because it shares 91% sequence identity with the human enzyme; human GAPDH is a potential target for the development of anti-apoptotic drugs. In addition, differences in the cofactor-binding pocket compared with the homology-model structure of GAPDH from the malaria parasite *Plasmodium falciparum* could be exploited in order to develop novel selective and potential antimalaria drugs.

1. Introduction

Phosphorylating D-glyceraldehyde-3-phosphate dehydrogenase (GAPDH; EC 1.2.1.12) is a ubiquitous enzyme essential for glycolysis, functioning as a homotetramer with a molecular mass of approximately 150 kDa. It catalyzes the oxidative phosphorylation of glyceraldehyde-3-phosphate (GAP) to 1,3-bisphosphoglycerate (BPG) using the cofactor NAD^+ (nicotinamide adenine dinucleotide). The first reaction step involves the formation of the hemiacetal intermediate between GAP and a cysteine residue. This hemiacetal intermediate is oxidized to a thioester, with concomitant reduction of NAD^+ to NADH. The reduced NADH is exchanged with the second NAD^+ molecule and the thioester is attacked by a nucleophilic inorganic phosphate to produce BPG (Harris & Waters, 1976).

Recent studies of mammalian GAPDH display a number of diverse activities unrelated to its glycolytic function (Sirover, 1999). These include the role of GAPDH in membrane fusion, microtubule bundling, phosphotransferase activity, nuclear RNA export, DNA replication and repair, apoptosis (Berry & Boulton, 2000; Tatton *et al.*, 2000), prostate cancer and viral pathogenesis. GAPDH also has been reported to be a target of nitric oxide (Sirover, 1999) and is implicated in neurodegenerative diseases such as Huntington's Disease (HD; Burke *et al.*, 1996), where polyglutamine-repeat-containing proteins bind to GAPDH. Involvement in Alzheimer's disease (AD) is assumed because GAPDH interacts with the β-amyloid precursor protein in amyloid plaques taken from AD brains (Schulze *et al.*, 1993).

Table 1
GAPDH structures in the PDB database.

Source	Ligands	Resolution (Å)	PDB code	Reference/comments/mutations
American lobster	NAD^+	2.9	1gpd	Moras *et al.* (1975)
(*Homarus americanus*)	NAD^+-free	2.8	4gpd	Murthy *et al.* (1980)
Chinese lobster	NAD^+	2.0	1szj	Song *et al.* (1998)
(*Palinurus versicolor*)	NAD^+	1.88	1dss	Song *et al.* (1999); carboxymethylated at Cys149
	NAD^+-free	2.0	1crw	Shen *et al.* (2000)
	ADP-ribose	3.0	1ihy	Shen *et al.* (2002)
	$SNAD^+$	2.8	1ihx	Shen *et al.* (2002)
Bacillus stearothermophilus	NAD^+	1.8	1gd1	Didierjean *et al.* (1997)
	NAD^+	2.5	1dbv	Skarzynski *et al.* (1987); D32G, L187A, P188S
	NAD^+	2.45	3dbv	Skarzynski *et al.* (1987); L33T, T34G, D36G, L187A, P188S
	NAD^+-free		2gd1	Skarzynski & Wonacott (1988)
	NADP	2.2	2dbv	Didierjean *et al.* (1997); D32G, L187A, P188S
		2.5	4dbv	Didierjean *et al.* (1997); L33T, T34G, D36G, L187A, P188S
Thermotoga maritima	NAD^+	2.5	1hdg	Korndorfer *et al.* (1995)
Thermus aquaticus	NAD^+	2.5	1cer	Tanner *et al.* (1996)
Sulfolobus solfataricus	NAD^+-free	2.05	1b7g	Isupov *et al.* (1999)
Escherichia coli	NAD^+	2.0	1dc6	Yun *et al.* (2000)
	NAD^+	1.8	1gad	Duee *et al.* (1996)
	NAD^+	2.17	1gae	Duee *et al.* (1996); N313T
	NAD^+-free	2.5	1dc3	Yun *et al.* (2000)
	NAD^+-free	2.0	1dc5	Yun *et al.* (2000)
	GAP substrate	2.5	1dc4	Yun *et al.* (2000); SeMet
Leishmania mexicana	NAD^+	2.8	1gyp	Kim *et al.* (1995)
	NAD^+	2.8	1a7k	Kim & Hol (1998)
	Inhibitor	3.4	1gyq	Aronov *et al.* (1999)
	Inhibitor	2.6	1i32	Suresh *et al.* (2001)
	Inhibitor	3.0	1i33	Suresh *et al.* (2001)
Trypanosoma brucei	NAD^+	3.2	1gga	Vellieux *et al.* (1993, 1995)
Trypanosoma cruzi	NAD^+	2.8	—	Souza *et al.* (1998)
	Inhibitor	1.95	1k3t	Pavao *et al.* (2002)
Duck (*Anas* sp.)	—	—	—	Barbosa (1996)
Methanothermus fervidus	NADP	2.1	1cf2	Charron *et al.* (2000)
Human skeletal muscle (*Homo sapiens*)	NAD^+	3.5	3gdp	Mercer *et al.* (1976), Watson *et al.* (1972)

High- and medium-resolution X-ray structures of NAD^+-bound GAPDH are available from various organisms (Table 1) and a low-resolution structure of GAPDH from human skeletal muscle has been determined (3.5 Å; PDB code 3gdp; Mercer *et al.*, 1976; Watson *et al.*, 1972).

Each subunit of the tetrameric enzyme is composed of two domains, *viz.* the NAD^+-binding domain and the catalytic domain. The active center is located in the interdomain area (Harris & Waters, 1976). The sequence and fold of the NAD^+-binding domains are conserved among various dehydrogenases, including lactate dehydrogenases and alcohol dehydrogenases. This fold, known as the Rossmann fold, has a central twisted parallel β-sheet surrounded by helices on both sides (Rossmann *et al.*, 1975). The catalytic domain consists of an eight-stranded mixed parallel β-sheet, with strands connected by short loops or α-helices. Structural, biochemical and mechanistic features of the enzyme have been reviewed recently (Nagradova, 2001). A recent publication describes the first structure of the hemiacetal intermediate of the glyceraldehyde-3-phosphate (GAP)–enzyme complex at atomic resolution (Yun *et al.*, 2000). In this structure, the C3 phosphate binds in a hydrophilic pocket called the P_i site. This result agrees with the flip-flop model proposed for the binding of GAP (Skarzynski *et al.*, 1987), in which the C3 phosphate of GAPDH initially binds to the P_i site during the formation of the hemiacetal intermediate and the C3 phosphate flips from the new P_i site to the P_s site before the hydride transfer. NAD^+ was not present in this hemiacetal structure. Only when the structure of the ternary complex containing both GAP and NAD^+ becomes available will it be possible to provide a complete description of the true binding site for GAP.

GAPDH has recently been identified as a mediator of apoptosis (Berry & Boulton, 2000; Tatton *et al.*, 2000). Antisense oligonucleotides against GAPDH rescue cells from apoptosis and (*R*)-deprenyl-related compounds bind to GAPDH and inhibit apoptosis. (*R*)-Deprenyl (Selegiline) is used in Parkinson's therapy to reduce neuronal cell death (Olanow *et al.*, 1995). The tricyclic deprenyl analog CGP3466 (dibenzo[*b*,*f*]oxepin-10-ylmethyl-methyl-prop-2-ynyl-amine; Kragten *et al.*, 1998) binds to and stabilizes a dimeric form of GAPDH and has a 100-fold inhibitory effect compared with deprenyl. CGP3466 (development name TCH346) is in phase II clinical trials as a drug responsible for neuroprotection in Parkinson's disease (Reed, 2002). The channel region of the tetrameric enzyme was described as the binding site of this compound (Carlile *et al.*, 2000; Tatton *et al.*, 2000). Here, we describe the crystal structure of rabbit (*Onyctolagus curniculum*) GAPDH, which was crystallized in the presence of CGP3466, and postulate a new binding site for this compound. To date, only a low-resolution structure (3.5 Å) of the human enzyme is available, which is 91% identical in sequence. The structure of rabbit-muscle GAPDH presented here at 2.4 Å resolution is the first medium-resolution three-dimensional structure of a mammalian GAPDH and provides an excellent basis for the design of compounds that inhibit the pro-apoptotic activity of human GAPDH.

Protozoan parasites cause millions of deaths every year. The protozoan parasite *Plasmodium falciparum*, which causes malaria, and the trypanosomatid parasites *Trypanosoma brucei* or *T. cruzi*, causing sleeping sickness or Chagas' disease, and *Leishmania mexicana*, causing leishmaniosis, do not possess an active citrate cycle; instead, ATP production in their bloodstream form depends fully on glycolysis (Sherman,

1998; Wang, 1995). Therefore, enzymes of the glycolytic pathway are attractive drug targets (Döbeli *et al.*, 1990; Verlinde *et al.*, 1994; Callens & Hannert, 1995; Hannert & Callens, 1995; Ridley, 1999; Bakker *et al.*, 2000; Daubenberger *et al.*, 2000). GAPDH is a highly conserved protein. Consequently, the slightest structural differences between the host and the parasite molecule are of interest when developing compounds that inhibit the parasite enzyme but not the human enzyme. So far, efforts have been concentrated on the development of compounds that inhibit the glycosomal form of the trypanosomatid GAPDH based on the three-dimensional structure (Hannert & Callens, 1995; Kennedy *et al.*, 2001). The structure of the mammalian GAPDH allows a precise description of the cofactor-binding-site differences between mammalian and parasitic GAPDHs that can be exploited for the development of selective and potent antiparasitic drugs. We also aimed at crystallizing the GAPDH from *P. falciparum* (pfGAPDH), a potential antimalarial drug target. Because crystals suitable for X-ray structure determination could not be grown, a homology model of pfGAPDH was constructed. The model was compared with the experimental rabbit-GAPDH structure and structural differences in the adenine-binding pocket were identified. These differences could be the basis for designing selective and potent antimalarial drugs.

2. Materials and methods

2.1. Protein preparation and crystallization

All chemicals were purchased from Fluka, except when indicated otherwise. GAPDH from rabbit muscle was obtained from Roche Diagnostics (Cat. No. 105 694) as a 10 mg ml^{-1} suspension in 3.2 *M* ammonium sulfate solution containing 0.1 m*M* EDTA pH 7.5. The protein was first diluted in 10 m*M* Tris–HCl pH 7.3, but protein crystallization experiments with this solution were unsuccessful. Dynamic light-scattering experiments (DynaPro-801 molecular-sizing instrument, Protein Solutions Ltd) were then performed in order to find conditions under which the protein solution was monodisperse and non-aggregated. 20 different buffer conditions were tested at both 277 and 293 K. Protein samples were first dialyzed overnight against the buffer in 100 µl dialysis disks (Hampton Research) and centrifuged before filtering the supernatant through 0.22 µm Millipore Ultrafree-MC centrifugal filter units. These experiments were all performed in the presence of a 100-fold excess of CGP3466. The Tris buffer of the original protein solution was then exchanged for 10 m*M* sodium cacodylate pH 6.5, which gave the lowest polydispersity measurements, and the protein solution was concentrated to 10 mg ml^{-1} before crystallization. Dynamic light-scattering experiments were also performed at concentrations up to 10 mg ml^{-1} and gave the same results (*i.e.* 87–88 kDa MW). These experiments were performed in order to confirm that the sodium cacodylate buffer was suitable for crystallization trials when the protein concentration was 10 mg ml^{-1}. Dynamic light-scattering experiments were also performed in the absence of CGP3466 for several of the buffers that gave low polydispersity values.

Rabbit GAPDH was crystallized by the sitting-drop vapor-diffusion method after microseeding of a drop equilibrated against 16%(*w*/*v*) PEG 3350, 0.1 *M* HEPES pH 8.0 and 0.2 *M* potassium citrate at a protein concentration of 10 mg ml^{-1}. Crystals grew as thin rods to a size of 1.0 × 0.08 × 0.02 mm.

2.2. Data collection and processing

Data collection was performed at 100 K using a cryoprotectant consisting of 25%(*v*/*v*) glycerol, 16%(*w*/*v*) PEG 3350, 0.1 *M* HEPES pH 8.0 and 0.16 *M* potassium citrate. Diffraction data were collected on a MAR Research imaging-plate system at the Swiss–Norwegian Beamline (SNBL) at the European Synchrotron Radiation Facility (ESRF) in Grenoble (France) from a single crystal at a wavelength of 0.8 Å. Data were processed with *DENZO*, *SCALEPACK* (Otwinowski & Wladek, 1996) and *TRUNCATE* (Collaborative Computational Project, Number 4, 1994). The space group is $P2_12_12_1$, with unit-cell parameters a = 81.70, b = 98.50, c = 183.10 Å. The asymmetric unit contains one GAPDH tetramer. The Matthews coefficient, V_M, is 2.48 Å^3 Da^{-1}, indicating an approximate solvent content of 50%. Merging of symmetry-related reflections resulted in 56 521 unique reflections and a multiplicity of 3.4 (3.3 in the last shell, 2.49–2.4 Å) with an R_{merge} value of 5.4% (20.6%). The completeness of the data to 2.4 Å was 96.6% (86.1%).

2.3. Structure determination

The crystal structure of rabbit GAPDH was solved by molecular replacement at 3.5 Å using the program *AMoRe* (Navaza, 1994). The coordinates of one dimer of *Bacillus stearothermophilus* GAPDH (Skarzynski *et al.*, 1987; PDB entry 1gd1) were used to build the initial search model. The top peaks in both the rotation and the translation functions were correct and the solutions were improved with rigid-body refinement at 3.5 Å to give a solution consisting of two dimers in the asymmetric unit, with a correlation coefficient of 43.2 and an R factor of 0.431.

2.4. Model building and crystallographic refinement

Manual fitting of the model to the electron density was carried out using the program *O* (Jones *et al.*, 1991). 4.9% of the reflections were randomly selected to create a data set of test reflections for cross-validation of the refinement procedure. The topology and parameter information for the NAD$^+$ cofactor and the *S*-oxyl Cys (CSX) were taken from the HIC-UP database (http://x-ray.bmc.uu.se/hicup/). The structure was refined in the resolution range 20–2.4 Å with the programs *X-PLOR* (Brünger, 1992; using protocols for rigid-body refinement, slow-cooling simulated annealing and minimization), *CNX* (http://www.accelrys.com/pdf/cnx/) and *CNS* (Brünger *et al.*, 1998; using torsion-angle molecular dynamics, slow-cooling simulated annealing and maximum-likelihood target function, energy minimization and individual *B*-factor refinement). The positions of water molecules were identified

with *CNS* and were checked manually. The crystal structure of rabbit GAPDH was refined using NCS (non-crystallographic symmetry) restraints on selected stretches of residues, which were identified by visual inspection of the four superimposed subunits in *O* (Jones *et al.*, 1991). The *R* factor of the final model is 20.32% and the free *R* factor is 23.85%. Structure validation was performed with the programs *PROCHECK* (Laskowski *et al.*, 1993) and *WHAT_CHECK* (Hooft *et al.*, 1997). Crystallographic statistics are given in Table 2.

Additional elongated density was observed in a cavity at the interface of the substrate-binding domain of each subunit (*O*, *P*, *Q*, *R*) and the NAD^+-binding domain of the neighboring subunit (*Q*, *R*, *O*, *P*) formed, for example, by Ser*O*273, Tyr*O*274, Asp*O*276, Phe*O*382, Asp*O*286, His*O*288 and residues Tyr*Q*46 and Lys*Q*52 from the neighboring monomer. This part of the electron-density map could represent a cluster of water molecules or a hypothetical ligand, which was either co-isolated from rabbit muscle or added in the buffers used for isolation. The surrounding residues would allow the formation of four hydrogen bonds to this water cluster or to an unidentified chemical compound. None of the substances used in the crystallization experiment would fit this electron-density distribution and the limited resolution did not allow interpretation of this density; therefore, five water molecules were modeled during the refinement. A number of charged surface side chains of the molecule are poorly resolved in all four subunits and electron density is weak or missing. Model building of a loop containing residue 25 in subunit *Q* was difficult because of weak electron density.

Table 2
Data-collection, data-processing and refinement statistics.

Values in parentheses refer to the highest-resolution shell.

Radiation source	Synchrotron
Beamline at ERSF	SNBL
Wavelength (Å)	0.8
Temperature (K)	100
Resolution range (Å)	2.0–2.4 (2.49–2.4)
No. of observations	194719
No. of unique reflections	56521
Data completeness (%)	96.6 (86.1)
Data redundancy	3.4 (3.3)
$R_{\rm merge}$ (%)	6.2 (22.7)
R factor (%)	20.3
$R_{\rm free}$ (%)	23.9
Average *B* factor (Å^2)	30.9
Average *B* factor (Å^2), NAD^+ molecules	72.7
Average *B* factor (Å^2), protein chains *O*, *P*, *Q*, *R*	30.3, 27.3, 32.5, 32.9
R.m.s.d., bond lengths (Å)	0.01
R.m.s.d., bond angles (°)	1.44
Solvent atoms	473
Ramachandran plot statistics (non-Pro and Gly residues), residues in	
Most favored regions	1016 (88.5%)
Additional allowed regions	124 (10.8%)
General allowed regions (Ala*O*/*P*/*Q*/*R*147)	4 (0.3%)
Disallowed regions (Val*O*/*P*/*Q*/*R*237)	4 (0.3%)
PROCHECK G factor	0.23

2.5. Homology modeling of GAPDH from *P. falciparum*

A multiple-sequence alignment procedure was carried out using *CLUSTALX* (Thompson *et al.*, 1994; Jeanmougin *et al.*, 1998). pfGAPDH shares more than 60% sequence identity with the human and the rabbit enzymes and 48% with the trypanosomatid glycosomal enzyme. pfGAPDH does not possess the loop insertion found in the glycosomal form of trypanosomatid GAPDH. All available GAPDH structures were superimposed with *SUPERIMPOSE* (Diederichs, 1995) and a structure-based sequence alignment was performed using *STRUPRO* (an *O*-related program; http://alpha2.bmc.uu.se/~gerard/; Kleywegt & Jones, 1998, 2001*a*,*b*). High- and medium-resolution structures of the NAD^+-bound form of American lobster (*Homarus americanus*; Moras *et al.*, 1975; PDB entry 1gpd), the Chinese lobster (*Palinurus versicolor*; Song *et al.*, 1998, 1999; PDB entries 1dss and 1szj) and rabbit GAPDH (present work) were used as templates for modeling pfGAPDH. 100 homology models were calculated using the program *MODELLER* and the subroutine *model* (Sali & Blundell, 1993; Sanchez & Sali, 2000). Each individual model was checked with the program *PROCHECK* (Laskowski *et al.*, 1993) from *CCP*4 (Collaborative Computational Project, Number 4, 1994) using a resolution of 3.0 Å. The homology model with the best stereochemistry was used for structure-comparison studies. A similar procedure generating a large number of models combined with a selection for the best sterochemistry has also been applied elsewhere (Kaufmann *et al.*, 2002).

3. Results and discussion

3.1. Preparation of rabbit-muscle GAPDH

CGP3466 (dibenzo[*b*,*f*]oxepin-10-ylmethyl-methyl-prop-2-ynyl-amine; Kragten *et al.*, 1998) inhibits the pro-apoptoic function of GAPDH (Carlile *et al.*, 2000; Tatton *et al.*, 2000) and is in phase II clinical trials for the treatment of neurodegeneration in Parkinson's disease (Reed, 2002). It has previously been shown that CGP3466 binds to isolated rabbit GAPDH (Kragten *et al.*, 1998) and converts the tetrameric GAPDH to the dimeric form (Carlile *et al.*, 2000; Tatton *et al.*, 2000). Commercially available rabbit GAPDH was diluted in 10 m*M* Tris–HCl at pH 7.3 in the presence of one molar excess of CGP3466 and reconcentrated to 10 mg ml^{-1} for crystallization screening. This preparation did not crystallize and was found to be highly polydisperse and to contain aggregates when analyzed by dynamic light scattering. Analysis of the protein incubated with a molar excess of CGP3466 in 20 different buffers at two different temperatures showed that measurements could be made for only 14 out of these 40 conditions, as a result of precipitation of the sample, and only three buffers gave a polydispersity of less than 15%. These buffers, sodium citrate pH 6.0 and sodium cacodylate pH 6.5 and 7.0, produced very similar values at both 277 and 293 K. In 0.1 *M* sodium cacodylate pH 6.5, which gives a polydispersity of 10% at 293 K, the estimated molecular weight is 90 kDa. This is roughly the size of a dimer of GAPDH (72 kDa), within the experimental error of extrapolating molecular weight from measurements of the hydrodynamic radius of the protein. In

the absence of CGP3466, the molecular weight was very similar, indicating that the dimer was also present and that CGP3466 did not have an effect on dimer formation in this buffer. Similar results were obtained with gel-filtration experiments (data not presented here). The slightly larger molecular weight could also be accounted for by the fact that there is probably a mixture of dimers and tetramers in solution, where the dimeric form dominates under the chosen buffer conditions. The protein was concentrated to 10 mg ml^{-1} in sodium cacodylate buffer pH 6.5 and used in crystallization experiments.

3.2. Crystallization

The GAPDH enzyme from rabbit muscle crystallized in space group $P2_12_12_1$, with a tetramer in the asymmetric unit, from a solution containing predominantly the dimeric form of the protein. Microseeding was necessary to produce single crystals, which grew as long needles from a solution at pH 8.0 containing polyethylene glycol as the precipitating agent. It seems that during the vapor-diffusion and concentration process in the crystallization experiment, the dimer/tetramer equilibrium was pushed towards the tetramer for crystal formation. The effect of CGP3466 in converting the oligomeric state to dimeric may have been hindered by the presence of active-site-bound NAD$^+$, as seen later in the structure. Diffraction data could be collected to 2.4 Å with the use of synchrotron radiation.

3.3. Structure determination and model description

The structure of rabbit-muscle GAPDH was solved by molecular replacement. The refined structure (using NCS restraints) has a final crystallographic R factor of 20.3% and an $R_{\rm free}$ of 23.9% at 2.4 Å resolution. NCS restraints were retained in the final model, as release of the restraints in a 'test' run of refinement led to a reduction in the R factor (to 18%), while the free R factor remained constant at about 24%, indicating overfitting of the model. There are only four non-glycine and non-proline residues (Val237 in all four chains) in the disallowed region of the Ramachandran plot. However, this residue has clear electron density in all four subunits and this combination of φ and ψ torsion angles is also found in this position in other GAPDH structures (*e.g.* PDB entries 1szj, 1gae and 1gd1). There are four monomers per asymmetric unit, designated O, P, Q and R, which form the tetrameric enzyme (nomenclature consistent with the PDB entry 1cer; Tanner *et al.*, 1996). The final model consists of 332 residues of each subunit (O, P, Q, R), two NAD$^+$ molecules and 474 water molecules. Crystallographic statistics are given in Table 2. The final $2F_o - F_c$ electron-density map shows well defined and continuous density for the entire GAPDH protein model (Fig. 1*a*).

Rabbit-muscle GAPDH has the same overall fold as all previously determined GAPDH structures. The four monomers in the asymmetric unit forming the tetramer are not identical (Fig. 2). The r.m.s.d. values of all C$^\alpha$ atoms are in the range 0.2–0.4 Å for the monomers, 0.3–0.5 Å for the NAD$^+$-binding domains (residues 1–147 and 312–332) and 0.1–0.2 Å for the catalytic domains (residues 148–311). One NAD$^+$ molecule per dimer of the tetrameric enzyme is bound to the monomers P and R (Figs. 1 and 3). This fact reflects the negative cooperativity in cofactor binding (Nagradova, 2001). The

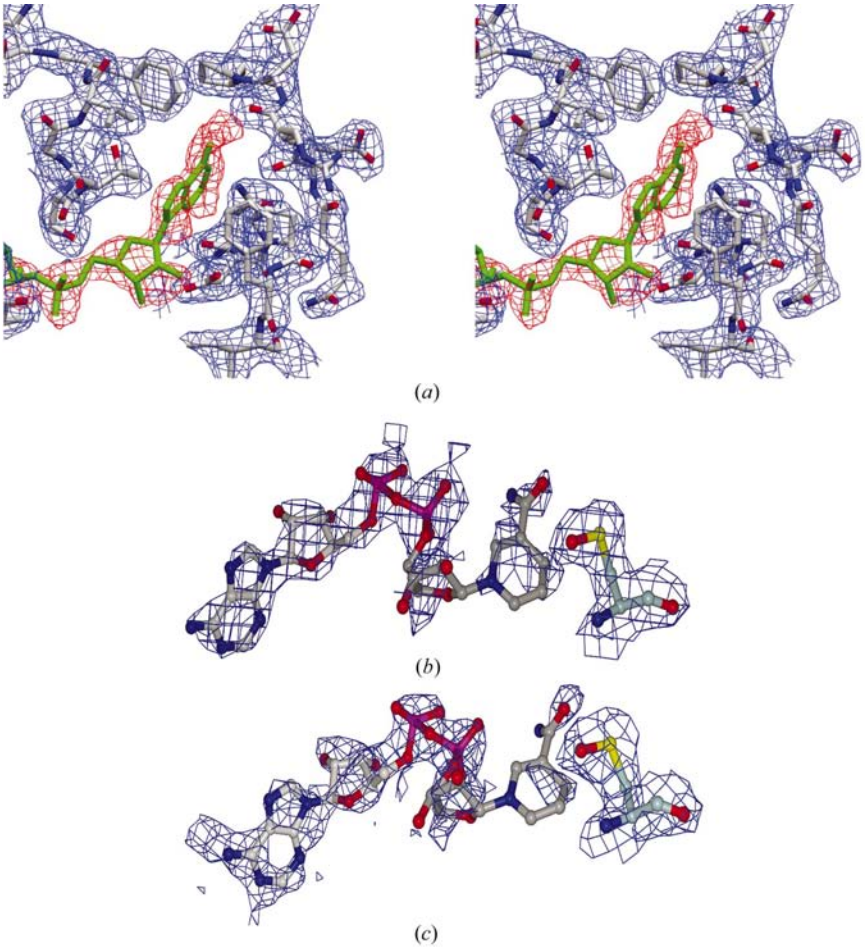

Figure 1
(*a*) Stereo representation of part of the rabbit GAPDH active site centered on the adenine part of the cofactor (subunit P). The omit map in red is contoured at 2.5σ and the electron density in blue ($2F_o - F_c$) is contoured at 1σ. The density for the cofactor in the omit map is almost identical to the density calculated from the $2F_o - F_c$ map shown in Figs. 1(*b*) and 1(*c*). (*b*, *c*) Electron density of the adenine part of the cofactor in subunits R (*b*) and P (*c*). The $2F_o - F_c$ electron density is contoured at 1.0σ (blue). The oxidized active-site cysteine is shown at the bottom of the figure. Incomplete electron density in the nicotinamide moiety is a consequence of higher flexibility of this part of the cofactor. The electron density is even weaker for this part of the cofactor bound to subunit P, either because of the lower occupancy or because of even higher flexibility. The figures were prepared using *DINO* (http://www.dino3d.org).

first two NAD^+ molecules bind with a higher affinity (K_d of about 0.01 μM) than the third and fourth NAD^+ molecules (K_d of 1–3 μM; Nagradova, 2001).

The NAD^+-bound and NAD^+-free subunits were superimposed and compared (Fig. 2). Binding of the NAD^+ cofactor forces a very slight movement from an open to a closed conformation. The largest differences are observed in loop regions close to the cofactor and are indicated by arrows in Fig. 2. The distance from the thiol group of the active-site Cys149 to the N^{ε} atom of the active-site His176 is reduced in the NAD^+-bound subunits *P* and *R* by 0.1 (not significant) and 0.4 Å, respectively, compared with the subunits *O* and *Q*. Similar rearrangements were reported for the GADPH structure of *B. stearothermophilus* (Skarzynski & Wonacott, 1988). The structure of the rabbit-muscle enzyme is the first GAPDH crystal structure in which both the holo and the apo form of the enzyme are present in one tetramer. When compared with the tetramer of GAPDH from *B. stearothermophilus* in the NAD^+-bound and NAD^+-free forms, the orientation of the NAD^+-free monomers is similar to the conformation of the *B. stearothermophilus* apo structure and the orientation of the NAD^+-bound monomers (especially the NAD^+-binding domain) adopts a conformation that is between the NAD^+-free and the NAD^+-bound form of the *B. stearothermophilus* enzyme.

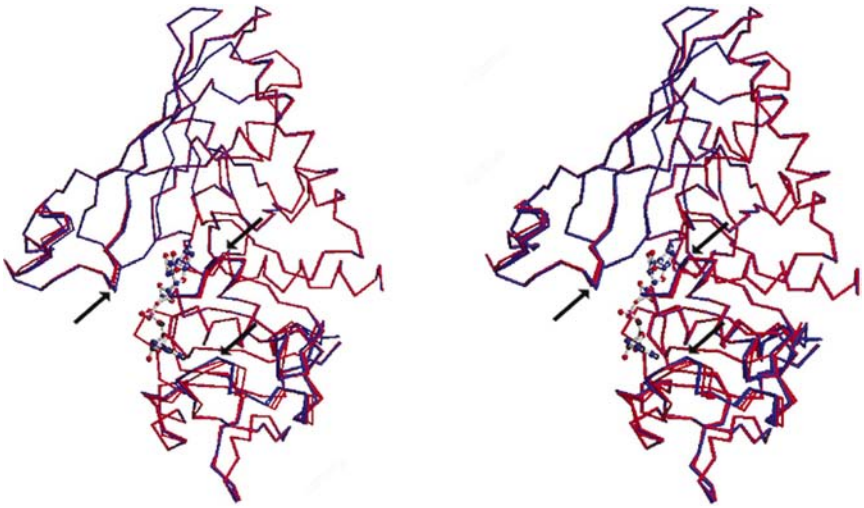

Figure 2
C^{α}-trace representation of rabbit GAPDH, showing a superposition of the four monomers. The NAD^+-free subunits, *O* and *Q*, are shown in red. The NAD^+-bound subunits, *P* and *R*, are colored blue. Subunit *R* is shown in complex with NAD^+. The arrows indicate loop regions close to the cofactor that are shifted towards NAD^+ when the cofactor is bound. The C^{α}-trace representation was prepared using *MOLSCRIPT* (Kraulis, 1991) and *Raster3D* (Merritt & Bacon, 1997).

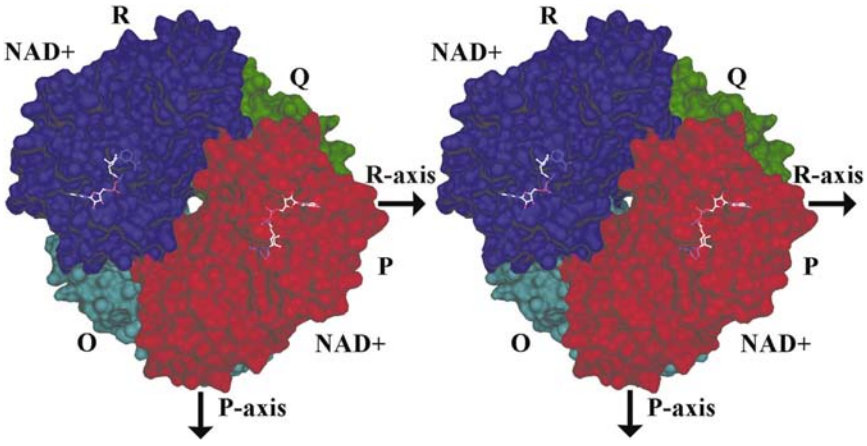

Figure 3
Surface representation of tetrameric rabbit GAPDH. One NAD^+ molecule is bound to each dimer of the tetrameric protein, namely to momomers *P* (blue) and *R* (red). The substrate-binding domain of chain *Q* (green) also contributes to the formation of the cofactor-binding cavity in chain *P* and the substrate-binding domain of chain *O* (cyan) contributes to the formation of the cofactor-binding cavity in chain *R*. The *P* and *R* axes of approximate 222 local symmetry are shown. The *Q* axis is located at the center of and parallel to the channel of the tetrameric enzyme (nomenclature following Buehner *et al.*, 1974). The molecular surface was calculated using *MSMS* (Sanner *et al.*, 1996) and the figure was prepared with *DINO* (http://www.dino3d.org).

3.3.1. Active site. The electron density indicates that the active-site cysteine (Cys149) residue is oxidized to sulfenic acid or *S*-oxyl Cys and refinement with *S*-oxyl Cys (CSX) gave an improvement of the final model. Oxidation of the active-site cysteine is a known phenomenon in GAPDH and has also been observed in GAPDH from *B. stearothermophilus* (Skarzynski *et al.*, 1987). Mass-spectrometry analysis (ESI-MS) of recombinant GAPDH from *P. falciparum* prepared as described by Daubenberger *et al.* (2000) revealed a mass 16 Da higher than the theoretical molecular mass of the GAPDH monomer, indicating that this protein was also oxidized. The catalytically important residue Arg231 (Nagradova, 2001) adopts a conformation that is unusual in GAPDH structures. The guanidinium group is shifted towards Asp195 and the Arg N^{ε} atom forms a hydrogen bond with the Asp carboxyl O atom. This hydrogen bond is responsible for the low pK_a value of about 9 reported for this side chain (Kuzminskaya *et al.*, 1991), which has previously been observed in the glycosomal GAPDH from *T. cruzi* (Souza *et al.*, 1998) where the corresponding residues are Arg249 and Asp210. The side chain of Asp195 in the rabbit enzyme is replaced by that of Arg195 in *B. stearothermophilus* GAPDH or glycine in the human enzyme.

3.3.2. Cofactor binding. NAD^+ molecules are bound in chains *P* and *R*, but they have relatively high temperature factors (Table 2). The atomic *B* factors for the adenine moiety are between 65 and 70 $Å^2$ and the atomic *B* factors for the nicotinamide part lie between 72 and 78 $Å^2$. The conformation of the adenine group in molecules *R* and *P* is

well defined (Fig. 1). Large temperature factors and fading electron density indicate that the nicotinamide part of the NAD^+ molecule possesses high flexibility. Because of the weak electron density in this region, an NAD^+ conformation known from homologous GAPDH structures was chosen for successful refinement.

In the cofactor-binding site of molecule *P*, the adenosine group fitted into the density, but negative $F_o - F_c$ difference density was observed after refinement in the center and positive difference density was observed at the edges of the adenine ring (Fig. 4*a*). These uncertainties in the electron density for the adenine moiety are a strong indication that another molecule is bound to the adenine-binding site with low occupancy. Since the compound CGP3466 was included in the crystallization experiment, we tried to fit it into the cavity of the adenine moiety (Fig. 4*b*). It has been shown previously that NAD^+ competes with CGP3466 binding (Kragten *et al.*, 1998). If NAD^+ and CGP3466 occupied the same binding site competition would be direct, but in the case where NAD^+ binding forces a conformational change of the CGP3466 pocket competition would be allosteric. Direct competition is supported by the fact that deprenyl, a CGP3466-related compound, binds to and inhibits the FAD-dependent monoamine oxidase B (Kwan *et al.*, 1995). It might be assumed that the deprenyl-like compound might bind to monoamine oxidase in a similar way as CGP3466 to GAPDH, as both enzymes are dinucleotide cofactor-dependent enzymes. Refinement of CGP3466 alone with reduced occupancy superimposed at the position of the adenine ring of the NAD^+ in subunit *P* did not improve the electron-density map significantly at this position. CGP3466 superimposed on to the adenine ring of the NAD^+ molecule in subunit *P* was then corefined with the NAD^+ molecule with *X-PLOR* (Brünger, 1992) (Fig. 4*c*). The occupancy of the cofactor was optimized to 70% for NAD^+ and 30% for the inhibitor. Two rings of CGP3466 are located at the position of the adenine group of the cofactor. The tricyclic analogue of deprenyl at the refined position is stabilized exclusively through hydrophobic interactions with nine neighboring residues. However, the electron density for CGP3466 is very weak and cannot be seen for all parts of the molecule. Therefore, additional experimental investigations are required to verify the binding mode of CGP3466. Carlile *et al.* (2000) proposed that the molecule binds to the channel of the tetrameric enzyme because the antibody-recognizing residues in the channel region of the tetrameic enzyme can block CGP3466 binding, but we cannot exclude the fact that the antibody used in this experiment reduced GCP3466 binding by a conformational change of the CGP3466-binding site that is distant from the channel region, *e.g.* the cofactor-binding cavity. Together, competition of NAD^+ and CGP3466, the fact that deprenyl binds to a related enzyme (monoamine oxidase B) and our structural analysis support binding of CGP3466 in the cavity for the adenine moiety of the NAD^+ cofactor.

Unconnected positive difference density was observed in the NAD^+-binding pocket of monomers *O* and *Q*, which was modeled as few water molecules. Water molecules were also identified in four out of eight of

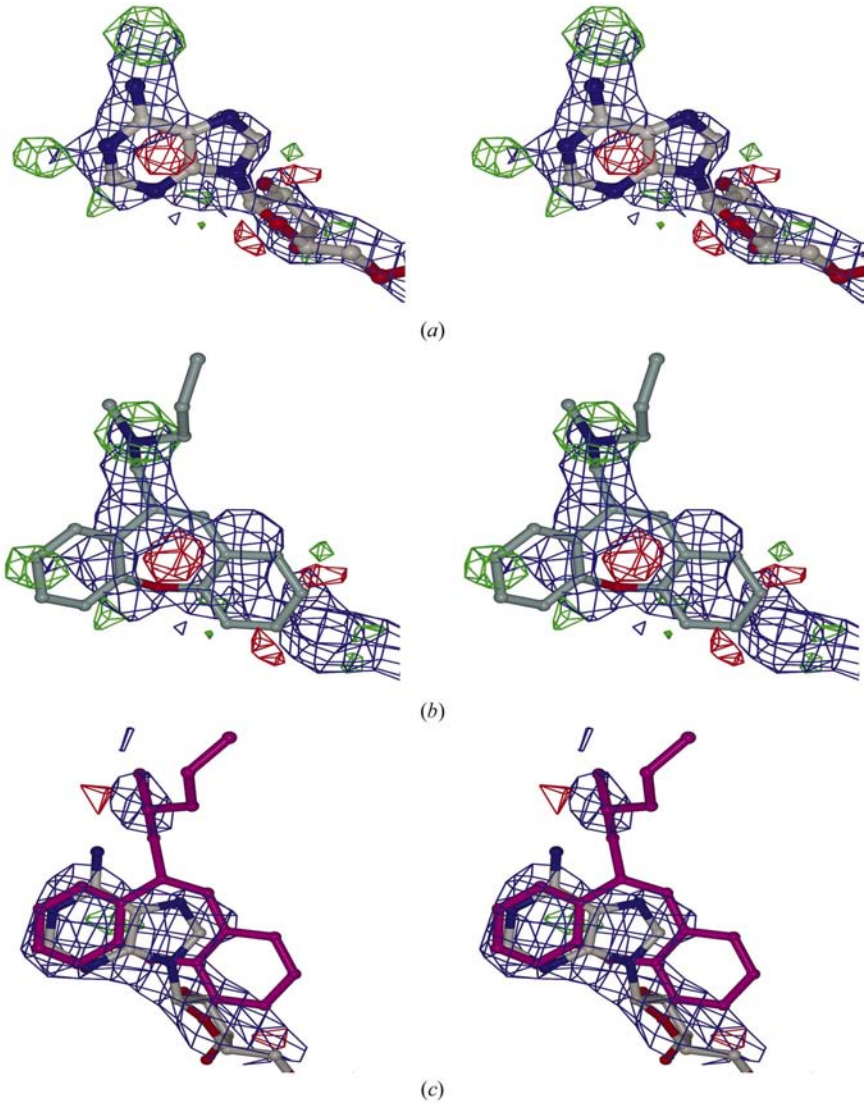

Figure 4
(*a*) Electron density of the adenine moiety of the cofactor in subunit *P*. The $2F_o - F_c$ electron density is contoured at 1.0σ (blue) and the $F_o - F_c$ electron density is contoured at $+3.0\sigma$ (green) and -3.0σ (red). Uncertainties in the electron density point towards the existence of another molecule bound at this site. (*b*) The compound CGP3466, placed at the position of the adenine ring prior to corefinement with NAD^+. Atoms are colored according to atom types (C grey, N blue, O red). (*c*) Electron-density map of the cofactor and CGP3466 (magenta) after corefinement in *X-PLOR*. The figures were prepared using *DINO* (http://www.dino3d.org).

Table 3
R.m.s.d. between the monomers and the NAD$^+$-binding domains of the crystal structure of rabbit GAPDH and the crystal structures of GAPDH from human (PDB code 3gpd), *L. mexicana* (1gyp), *E. coli* (1gad or 1dc6), American lobster (1gpd) Chinese lobster (1szj) and the homology model of *P. falciparum*.

The r.m.s.d. values of all C$^\alpha$ atoms were calculated with the *DALI* server (Holm & Sander, 1993; http://www.ebi.ac.uk/dali/).

	L. mexicana (358 residues)	*E. coli* (330 residues)	American lobster (333 residues)	Chinese lobster (333 residues)	*P. falciparum* (337 residues)
Rabbit GAPDH monomer *R* (332 residues)	1.2 Å for 332 C$^\alpha$ atoms	0.7 or 0.8 Å for 328 C$^\alpha$ atoms	1.3 Å for 330 C$^\alpha$ atoms	0.5 Å for 331 C$^\alpha$ atoms	1.3 Å for 330 C$^\alpha$ atoms
Rabbit GAPDH NAD$^+$-binding domain (168 residues of monomer *R*)	1.3 Å for 167 C$^\alpha$ atoms	0.9 Å for 163 or 164 C$^\alpha$ atoms	1.1 Å for 167 C$^\alpha$ atoms	0.5 Å for 1 67 C$^\alpha$ atoms	1.1 Å for 167 C$^\alpha$ atoms

the putative phosphate-binding sites (P_i and P_s) in the tetrameric enzyme.

3.4. Structural comparison

Comparison of the rabbit-GAPDH structure with the GAPDH structures from other organisms shows that the overall fold is highly conserved. The r.m.s.d. values of the C$^\alpha$ atoms [calculated with the *DALI* (Holm & Sander, 1993) server; http://www.ebi.ac.uk/dali/] between monomers from the different species are listed in Table 3. Higher structural variability of the glycosomal enzymes of the trypanosomatid protozoa (*e.g. L. mexicana*) in loop regions with sequence insertions is not reflected in the r.m.s.d., as the r.m.s.d. is only calculated for aligned residues (Fig. 5). Our homology model of *P. falciparum* was also included in this comparison. The residues involved in catalysis and phosphate binding are highly conserved. The 2.4 Å rabbit GAPDH structure and the 3.5 Å human GAPDH structure are also highly conserved. The residues involved in NAD$^+$ binding are identical in both the rabbit and the human enzyme, except for the single residue Gln6 in the rabbit enzyme, which is replaced by Asp in the human homolog. Therefore, the structure of rabbit GAPDH represents an excellent starting point for the structure-based design of anti-apoptotic drugs.

Glycosomal GAPDH from trypanosomatid parasites was identified as a potential drug target because significant differences in the cavity forming the binding site of the adenine ring of the NAD$^+$ cofactor were identified when the human enzyme was compared with glycosomal GAPDH from *L. mexicana*, *T. cruzi* and *T. brucei* (Suresh *et al.*, 2001). Adenosine and NAD$^+$ homologues have been synthesized that inhibit the trypanosomatid GAPDH significantly more strongly than the human enzyme (Bressi *et al.*, 2001; Kennedy *et al.*, 2001). The cavity involved in binding the adenine moiety of the cofactor is formed by the NAD$^+$-binding domain (*e.g.* subunit *R*) and by residues of the catalytic domain of a neighboring monomer (*e.g.* subunit *O*). When the rabbit structure is compared with the *L. mexicana* enzyme and *P. falciparum* enzyme model structures, striking differences are detected (Fig. 6).

Suresh *et al.* (2001) found that the residue homologous to Gly192 in human GAPDH is mutated to Leu208 in the trypanosomatid glycosomal enzyme. In the rabbit enzyme, the corresponding residue is Gly190. This residue is close to the adenine part of the cofactor. In the plasmodium GAPDH model structure, an insertion of the three amino acids Lys, Gly and Gly occurs at the position of Gly190 in the human and rabbit structures. In the homology model, the lysine side chain is found in the position of the valine (*L. mexicana* enzyme) or the glycine (rabbit or human protein). In addition, in the plasmodium protein there is a methionine in place of Ile35 (rabbit GAPDH), which makes the pocket close to O-2′ of the adenine ribose smaller. The precise conformation of the inserted residues and the conformation of the lysine could not

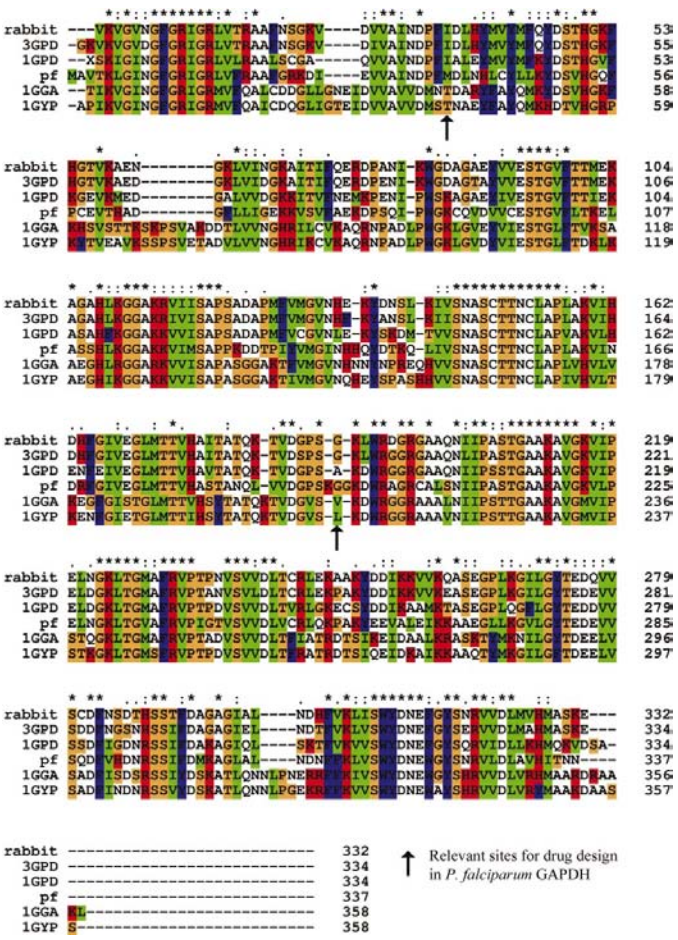

Figure 5
Structure-based sequence alignment of *P. falciparum* (pf), *T. brucei* (1GAA), *L. mexicana* (1GYP), human (3GPD), rabbit and American lobster (1GPD) GAPDH.

be modeled very accurately. The determination of the three-dimensional structure of the plasmodium enzyme would provide the precise architecture of the NAD^+ cavity formed by the catalytic domain of the neighboring monomer and would be a better basis for the structure-based design of antimalaria drugs.

4. Conclusions

The rabbit-muscle GAPDH crystal structure has been determined at 2.4 Å resolution. Dynamic light-scattering experiments were necessary to identify an appropriate buffer for crystallization screening. One NAD^+ molecule is bound to each dimer in the tetrameric enzyme, consistent with the described negative cooperativity for NAD^+ binding. The uncertainties in the electron-density map for the NAD^+ adenine moiety in subunit *P* together with literature data strongly indicate that the anti-apoptotic compound CGP3466 binds in this pocket and not in the channel formed by the tetramer. The present structure could help in the design of new drugs inhibiting the pro-apoptotic activity of the GAPDH. In addition, differences in the cofactor-binding site revealed by a comparison of the mammalian GAPDH with GAPDH of *P. falciparum* could be exploited to develop more efficient antimalaria drugs.

Experimental assistance from the staff of the Swiss–Norwegian beamline at the European Synchrotron Radiation Facility is gratefully acknowledged. The authors thank the Swiss Tropical Institute in Basel, Gerd Pluschke and Claudia Daubenberger for stimulating discussions on pfGAPDH, Marija Curcic and Frederike Pöltl-Frank for preparing recombinant pfGAPDH, and the Protein Analysis Unit of the Institute of Biochemistry, University of Zurich for performing mass-spectrometry analysis. The authors also thank Jean-Michel Rondeau, Sylvie Raccuglia and Francis Bitsch for help with analytical studies of rabbit GAPDH, and Guido Capitani, Peter Waldmeier and Kaspar Zimmermann for stimulating discussions. The financial support of the Baugartenstiftung (CH-8022 Zürich) and a grant from the Swiss National Science Foundation to MGG are gratefully acknowledged.

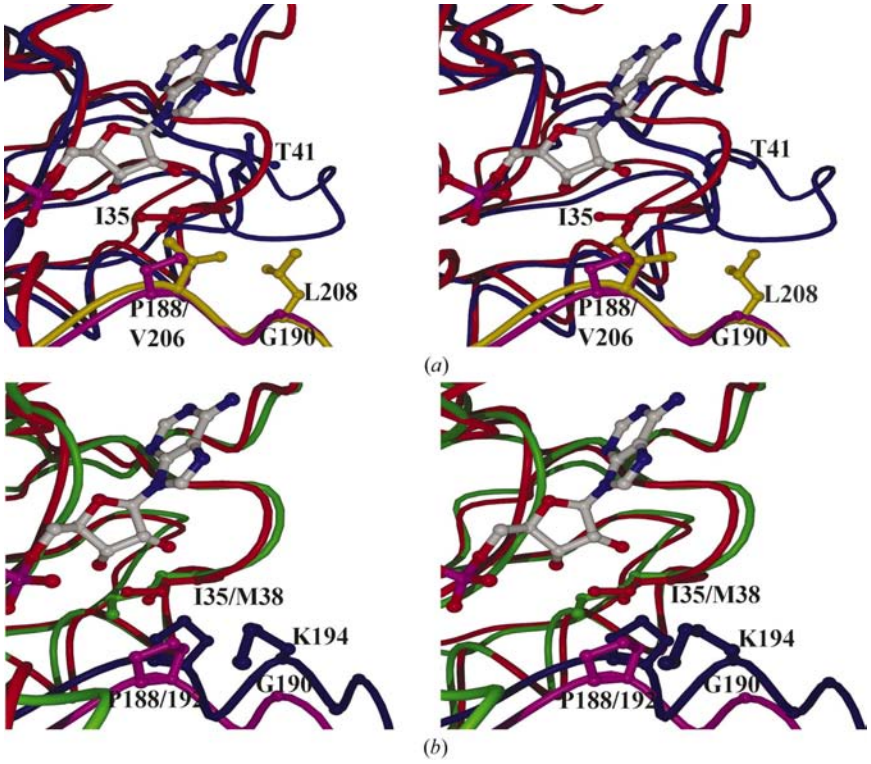

Figure 6
Details of the cofactor-binding pocket in GAPDH. The backbone of the NAD^+-binding domain of chain *R* from rabbit GAPDH is colored red. The backbone of the substrate-binding domain of the neighboring subunit is colored magenta. The adenine moiety of the NAD^+ cofactor of rabbit GAPDH (chain *R*) is shown in ball-and-stick form, as are the side chains of the residues marked by an arrow in Fig. 5. (*a*) Comparison of the rabbit structure with the crystal structure of GAPDH from *L. mexicana* (PDB code 1gyp). The side chains displayed have been identified (among others) as being different in *L. mexicana* GAPDH and the rabbit enzyme and are therefore thought to be of relevance for drug design. The NAD^+-binding domain of *L. mexicana* GAPDH is shown in blue and the substrate-binding domain of the neighboring subunit is colored yellow. (*b*) Comparison of the rabbit structure with the homology model of GAPDH from *P. falciparum*, based on a superposition of the NAD^+-binding domains (green for pfGAPDH). The neighboring substrate-binding domain of the pfGAPDH model is shown in blue. The proline at position 188 in the rabbit structure is conserved in *P. falciparum* GAPDH (residue number 190). Gly190 in rabbit is replaced by KGG in pfGAPDH. This insertion and especially the lysine side chain seem to close the cavity between the cofactor and the neighboring subunit.

References

Aronov, A. M., Suresh, S., Buckner, F. S., Van Voorhis, W. C., Verlinde, C. L., Opperdoes, F. R., Hol, W. G. & Gelb, M. H. (1999). *Proc. Natl Acad. Sci. USA*, **96**, 4273–4278.

Bakker, B. M., Westerhoff, H. V., Opperdoes, F. R. & Michels, P. A. (2000). *Mol. Biochem. Parasitol.* **106**, 1–10.

Barbosa, V. M. (1996). PhD Thesis. University of Sao Paulo, Brazil.

Berry, M. D. & Boulton, A. A. (2000). *J. Neurosci. Res.* **60**, 150–154.

Bressi, J. C., Verlinde, C. L., Aronov, A. M., Shaw, M. L., Shin, S. S., Nguyen, L. N., Suresh, S., Buckner, F. S., Van Voorhis, W. C., Kuntz, I. D., Hol, W. G. & Gelb, M. H. (2001). *J. Med. Chem.* **44**, 2080–2093.

Brünger, A. T. (1992). *X-PLOR Version 3.1*. Yale University Press, New Haven, CT, USA.

Brünger, A. T., Adams, P. D., Clore, G. M., DeLano, W. L., Gros, P., Grosse-Kunstleve, R. W., Jiang, J.-S., Kuszewski, J., Nilges, M., Pannu, N. S., Read, R. J., Rice, L. M., Simonson, T. & Warren, G. L. (1998). *Acta Cryst.* D**54**, 905–921.

Buehner, M., Ford, G. C., Moras, D., Olsen, K. W. & Rossmann, M. G. (1974). *J. Mol. Biol.* **82**, 563–585.

Burke, J. R., Enghild, J. J., Martin, M. E., Jou, Y. S., Myers, R. M., Roses, A. D., Vance, J. M. & Strittmatter, W. J. (1996). *Nature Med.* **2**, 347–350.

Callens, M. & Hannert, V. (1995). *Ann. Trop. Med. Parasitol.* **89**, 23–30.

Carlile, G. W., Chalmers-Redman, R. M., Tatton, N. A., Pong, A., Borden, K. E. & Tatton, W. G. (2000). *Mol. Pharmacol.* **57**, 2–12.

Charron, C., Talfournier, F., Isupov, M. N., Littlechild, J. A., Branlant, G., Vitoux, B. & Aubry, A. (2000). *J. Mol. Biol.* **297**, 481–500.

Collaborative Computational Project, Number 4 (1994). *Acta Cryst.* D**50**, 760–763.

Daubenberger, C. A., Pöltl-Frank, F., Jiang, G., Lipp, J., Certa, U. & Pluschke, G. (2000). *Gene*, **246**, 255–264.

Didierjean, C., Rahuel-Clermont, S., Vitoux, B., Dideberg, O., Branlant, G. & Aubry, A. (1997). *J. Mol. Biol.* **268**, 739–759.

Diederichs, K. (1995). *Proteins*, **23**, 187–195.

Döbeli, H., Trzeciak, A., Gillessen, D., Matile, H., Srivastava, I. K., Perrin, L. H., Jakob, P. E. & Certa, U. (1990). *Mol. Biochem. Parasitol.* **41**, 259–268.

Duee, E., Olivier-Deyris, L., Fanchon, E., Corbier, C., Branlant, G. & Dideberg, O. (1996). *J. Mol. Biol.* **257**, 814–838.

Hannert, V. & Callens, M. (1995). *Ann. Trop. Med. Parasitol.* **89**, 23–30.

Harris, J. I. & Waters, M. (1976). *The Enzymes*, 3rd ed., edited by P. D. Boyer, ch. 13. New York: Academic Press.

Holm, L. & Sander, C. (1993). *J. Mol. Biol.* **233**, 123–138.

Hooft, R. W., Vriend, G., Sander, C. & Abola, E. E. (1997). *Nature* (*London*), **381**, 272.

Isupov, M. N., Fleming, T. M., Dalby, A. R., Crowhurst, G. S., Bourne, P. C. & Littlechild, J. A. (1999). *J. Mol. Biol.* **291**, 651–660.

Jeanmougin, F., Thompson, J. D., Gouy, M., Higgins, D. G. & Gibson, T. J. (1998). *Trends Biochem. Sci.* **23**, 403–405.

Jones, T. A., Zou, J. Y., Cowan, S. W. & Kjeldgaard, M. (1991). *Acta Cryst.* A**47**, 110–119.

Kaufmann, M., Bozic, D., Briand, C., Bodmer, J. L., Zerbe, O., Kohl, A., Tschopp, J. & Grütter, M. G. (2002). *FEBS Lett.* **527**, 250–254.

Kennedy, K. J., Bressi, J. C. & Gelb, M. H. (2001). *Bioorg. Med. Chem. Lett.* **11**, 95–98.

Kim, H., Feil, I. K., Verlinde, C. L., Petra, P. H. & Hol, W. G. (1995). *Biochemistry*, **34**, 14975–14986.

Kim, H. & Hol, W. G. (1998). *J. Mol. Biol.* **278**, 5–11.

Kleywegt, G. J. & Jones, T. A. (1998). *Acta Cryst.* D**54**, 1119–1131.

Kleywegt, G. J. & Jones, T. A. (2001*a*). *International Tables for Crystallography*, Vol. *F*, edited by M. G. Rossmann & E. Arnold, pp. 353–356. Dordrecht: Kluwer Academic Publishers.

Kleywegt, G. J. & Jones, T. A. (2001*b*). *International Tables for Crystallography*, Vol. *F*, edited by M. G. Rossmann & E. Arnold, pp. 366–367. Dordrecht: Kluwer Academic Publishers.

Korndorfer, I., Steipe, B., Huber, R., Tomschy, A. & Jaenicke, R. (1995). *J. Mol. Biol.* **246**, 511–521.

Kragten, E., Lalande, I., Zimmermann, K., Roggo, S., Schindler, P., Müller, D., van Oostrum, J., Waldmeier, P. & Fürst, P. (1998). *J. Biol. Chem.* **273**, 5821–5828.

Kraulis, P. J. (1991). *J. Appl. Cryst.* **24**, 946–950.

Kuzminskaya, E. V., Asryants, R. A. & Nagradova, N. K. (1991). *Biochim. Biophys. Acta*, **1075**, 123–130.

Kwan, S. W., Lewis, D. A., Zhou, B. P. & Abell, C. W. (1995). *Arch. Biochem. Biophys.* **316**, 385–391.

Laskowski, R. A., MacArthur, M. W., Moss, D. S. & Thornton, J. M. (1993). *J. Appl. Cryst.* **26**, 283–291.

Mercer, W. D., Winn, S. I. & Watson, H. C. (1976). *J. Mol. Biol.* **104**, 277–283.

Merritt, E. A. & Bacon, D. J. (1997). *Methods Enzymol.* **277**, 505–524.

Moras, D., Olsen, K. W., Sabesan, M. N., Buehner, M., Ford, G. C. & Rossmann, M. G. (1975). *J. Biol. Chem.* **250**, 9137–9162.

Murthy, M. R., Garavito, R. M., Johnson, J. E. & Rossmann, M. G. (1980). *J. Mol. Biol.* **138**, 859–872.

Nagradova, N. K. (2001). *Biochemistry* (*Moscow*), **66**, 1067–1076.

Navaza, J. (1994). *Acta Cryst.* A**50**, 157–163.

Olanow, C. W., Hauser, R. A., Gauger, L., Malapira, T., Koller, W., Hubble, J., Bushenbark, K., Lilienfeld, D. & Esterlitz, J. (1995). *Ann. Neurol.* **38**, 771–777.

Otwinowski, Z. & Wladek, M. (1996). *Methods Enzymol.* **276**, 307–326.

Pavao, F., Castilho, M. S., Pupo, M. T., Dias, R. L., Correa, A. G., Fernandes, J. B., da Silva, M. F., Mafezoli, J., Vieira, P. C. & Oliva, G. (2002). *FEBS Lett.* **520**, 13–17.

Reed, J. C. (2002). *Nature Rev. Drug Discov.* **1**, 111–121.

Ridley, R. G. (1999). *Science*, **285**, 1502–1503.

Rossmann, M. G., Liljas, A., Brändén, C. I. & Banaszak. (1975). *The Enzymes*, 3rd ed., edited by P. D. Boyer, ch. 13. New York: Academic Press.

Sali, A. & Blundell, T. L. (1993). *J. Mol. Biol.* **234**, 779–815.

Sanchez, R. & Sali, A. (2000). *Methods Mol. Biol.* **143**, 97–129.

Sanner, M. F., Olson, A. J. & Spehner, J. C. (1996). *Biopolymers*, **38**, 305–320.

Schulze, H., Schuler, A., Stuber, D., Dobeli, H., Langen, H. & Huber, G. (1993). *J. Neurochem.* **60**, 1915–1922.

Shen, Y. Q., Li, J., Song, S. Y. & Lin, Z. J. (2000). *J. Struct. Biol.* **130**, 1–9.

Shen, Y. Q., Song, S. Y. & Lin, Z. J. (2002). *Acta Cryst.* D**58**, 1287–1297.

Sherman, I. W. (1998). Editor. *Malaria: Parasite Biology, Pathogenesis and Protection*, pp. 135–143. Washington DC: ASM Press.

Sirover, M. A. (1999). *Biochim. Biophys. Acta*, **1432**, 159–184.

Skarzynski, T., Moody, P. C. & Wonacott, A. J. (1987). *J. Mol. Biol.* **193**, 171–187.

Skarzynski, T. & Wonacott, A. J. (1988). *J. Mol. Biol.* **203**, 1097–1118.

Song, S., Li, J. & Lin, Z. (1998). *Acta Cryst.* D**54**, 558–569.

Song, S. Y., Xu, Y. B., Lin, Z. J. & Tsou, C. L. (1999). *J. Mol. Biol.* **287**, 719–725.

Souza, D. H., Garratt, R. C., Araujo, A. P., Guimaraes, B. G., Jesus, W. D., Michels, P. A., Hannaert, V. & Oliva, G. (1998). *FEBS Lett.* **424**, 131–135.

Suresh, S., Bressi, J. C., Kennedy, K. J., Verlinde, C. L., Gelb, M. H. & Hol, W. G. (2001). *J. Mol. Biol.* **309**, 423–435.

Tanner, J. J., Hecht, R. M. & Krause, K. L. (1996). *Biochemistry*, **35**, 2597–2609.

Tatton, W. G., Chalmers-Redman, R. M., Elstner, M., Leesch, W., Jagodzinski, F. B., Stupak, D. P., Sugrue, M. M. & Tatton, N. A. (2000). *J. Neural Transm. Suppl.* **60**, 77–100.

Thompson, J. D., Higgins, D. G. & Gibson, T. J. (1994). *Nucleic Acids Res.* **22**, 4673–4680.

Vellieux, F. M. *et al.* (1993). *Proc. Natl Acad. Sci. USA*, **90**, 2355–2359.

Vellieux, F. M., Hajdu, J. & Hol, W. G. (1995). *Acta Cryst.* D**51**, 575–589.

Verlinde, C. L., Merritt, E. A., Van den Akker, F., Kim, H., Feil, I., Delboni, L. F., Mande, S. C., Sarfaty, S., Petra, P. H. & Hol, W. G. (1994). *Protein Sci.* **3**, 1670–1686.

Wang, C. C. (1995). *Ann. Rev. Pharmacol. Toxicol.* **35**, 93–127.

Watson, H. C., Duee, E. & Mercer, W. D. (1972). *Nature New Biol.* **240**, 130–133.

Yun, M., Park, C. G., Kim, J. Y. & Park, H. W. (2000). *Biochemistry*, **39**, 10702–10710.